Linear stability analysis of a submerged cylinder

Leo M. González, Esteban Ferrer
Technical University of Madrid (UPM)
Arco de la Victoria 4, 28040 Madrid, Spain

Juan M. Gimenez
Centro de Investigación de Métodos Computacionales (CIMEC) - UNL/CONICET
Facultad de Ingeniería y Ciencias Hídricas - Universidad Nacional del Litoral
Paraje El Pozo, Santa Fe, Argentina
(Dated: July 20, 2016)

This Letter describes how the global stability analysis of a circular cylinder is affected when submerged in a two phase gravitational flow. The flow behavior is governed by both the Reynolds and Froude numbers, while the depth of the cylinder has been varied to create different scenarios for the stability analysis. The baseflow obtained by the Navier-Stokes equations has been analyzed, and the first bifurcation (i.e. Hopf type) has been obtained for a fixed Froude number. The critical Reynolds number and the frequency of the most unstable mode have been compared to the classical solution without free surface and gravity effects. The most unstable mode is deformed and distorted according to the free surface location, while the critical Reynolds numbers and frequency are both affected by the gravity and the free surface presence.

INTRODUCTION

The interaction between the viscous wake of a submerged object and the free surface position is a problem that deserves attention. Several reasons sustain its importance, [1] justifies the study due to its potential relevance for the remote sensing of the ocean surface from satellites, while [2, 3] outline its application to the design of offshore structures and vessels. It is well known that in the absence of free surface and gravity, the von Kármán vortex street generated by flow past an infinitely long circular cylinder produces a two dimensional time periodic flow for Reynolds numbers between approximately 47 and 189 [4–7]. This work focuses on the changes produced in the stability of this flow when the cylinder is submerged and a free surface separating two different fluids in the presence of gravity. Different steady baseflows have been studied and a linear global stability analysis has been performed in order to quantify the differences when free surface and gravity are added to the problem. Previous authors performed stability analysis of idealized problems such as simple vortex structures [8, 9] and analytic shear flows [1]. To the authors knowledge, this constitutes the first study where a global stability analysis is performed on a Navier-Stokes computed solution in the presence of high discontinuities in density caused by the free surface. In order to gain insight about the physics of the interaction, the limits of steady solution where the velocity, the pressure and the free surface finally reach a stationary state are analyzed. The problem depends on two non-dimensional numbers, the Reynolds and the Froude numbers and one geometrical parameter which is the cylinder depth. The classical case when, in the absence of gravity only one fluid is used has a very well studied solution and the steady separation bubble breaks its symmetry (i.e. becoming unstable) when the only non-dimensional parameter, increases its value above $Re_c \approx 47$(based on the cylinder diameter). For Reynolds numbers above this critical value, perturbations amplify and the de-stability the separation bubble. In our study the Reynolds number has been increased from subcritical to supercritical values while the Froude number based on the cylinder diameter has been kept constant along the study for three different cylinder depths. Two causes could trigger the first instability of these flows: typical vortex shedding instability or a free surface Rayleigh-Taylor instability. In our study the range of parameters Reynolds, Froude and cylinder depth has been selected such that the vortex shedding is the cause of instability while free surface instabilities are not considered due to the fluid setup where the heavier is placed at the bottom. This hypothesis is confirmed by the Dynamic Mode Decomposition (DMD)[15] technique, which is performed on the supercritical range. The latter analysis did not reveal any dominant free-surface instability and showed that vortex shedding modes are well captured through the linear stability analysis of the mean flow. Similarly to the work presented by Triantafyllou and Dimas [1], the purpose here is to analyze the stability of the wake of floating two-dimensional objects. However, a few differences can be found between the two methodologies. First, in our case no analytic hypothesis of the flow or weakly parallel assumptions have been used for the baseflow construction, instead, the base flow has been computed solving the Navier-Stokes equations for both fluids. Second, no boundary conditions have been used for the free surface, and a scalar Volume Of Fluid (VOF) function[10] has been added to the simulation to represent density and viscosity changes. Third, a two dimensional global analysis has been performed, and consequently we have not assumed any harmonic dependance

of the perturbation in the flow direction (e.g. parallel flow).

METHODOLOGY

The governing equations are the incompressible Navier–Stokes equations in laminar regime, which are supplemented with the conventional boundary conditions on solid and/or open boundaries. The computational domain Ω contains both fluids, the first one (denoted by subscript 1) is placed at the top of the domain and the second at the bottom (subscript 2). Let us name their corresponding densities and kinematic viscosities as ρ_i and ν_i $(i = 1, 2)$, respectively, where $\rho_2 \gg \rho_1$. The non dimensional governing equations, written in a Lagrangian framework, are:

$$\nabla \cdot (\frac{1}{\beta}\mathbf{v}) = 0, \tag{1}$$

$$\frac{D\mathbf{v}}{Dt} = -\beta\nabla p + \nabla \cdot (\alpha\nabla\mathbf{v}) + \frac{1}{Fr_D^2}\mathbf{u_g}. \tag{2}$$

Here $\mathbf{v}$, p are the velocity and fluid pressure and $\mathbf{u_g}$ is a unitary vector parallel to the gravity force. The equations are computed in non-dimensional form using the cylinder diameter D, the inflow velocity U and the density and viscosity of the bottom fluid such that Reynolds $Re_D = \frac{UD}{\nu_2}$ and Froude $Fr_D = \frac{U}{\sqrt{gD}}$ numbers are defined using the properties of the bottom fluid. It is important to remark that compared to the case where only one fluid is involved, two non dimensional coefficients α and β (both specially relevant when including the free surface interface) appear explicitly in the mass and momentum conservation equations (1) and (2).

$$\alpha = \frac{(\phi+1) - (\frac{\nu_1}{\nu_2})(\phi-1)}{2Re_D}, \tag{3}$$

$$\frac{1}{\beta} = \frac{(\phi+1)}{2} - \frac{\rho_1}{\rho_2}\frac{(\phi-1)}{2}, \tag{4}$$

where ϕ is the scalar function such that: $\phi = -1$ in the fluid 1 and $\phi = 1$ in the fluid 2. As usual, the free surface is represented by VOF function isosurface $\phi = 0$. An efficient and accurate methodology Particle Finite Element Method (PFEM-2)[11] has been used to numerically simulate the dynamics of the incompressible baseflows. It is important to remark that both density and viscosity are discontinuous functions that are accurately transported according to the techniques described in [11]. We choose a sufficiently large domain to minimize undesirable boundary effects. The inflow and exit boundaries are located at 18D and 35D upstream and downstream of the cylinder, respectively. Side boundaries are at 15D apart from the central axis. A uniform inflow boundary condition, together with a natural boundary condition for the far field and outflow, are applied for the velocity. No-slip boundary conditions are employed for cylinder walls. A Neumann boundary condition is imposed for the pressure in all boundaries except the outflow where zero Dirichlet condition is imposed. Details are provided in FIG. 1.

After a complete mesh converge process based on the drag and lift forces, a final mesh has been retained. The mesh used for the simulations is a triangular mesh that contains 65834 triangles and 132542 nodes, the default mesh size is 0.655D while in the cylinder proximities and the free surface region, the mesh size has been refined to 0.0016D.

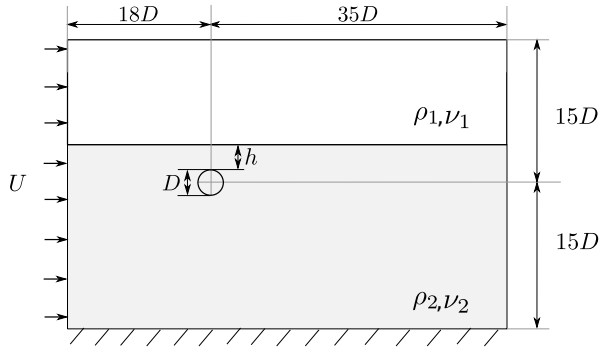

FIG. 1: Computational domain description for baseflow computation and subsequent stability analysis.

An accurate simulation of the interface evolution is crucial when simulating free-surface flows. During the flow evolution, it is essential that the interface remains sharp. Large jumps of fluid density and viscosity across the interface should be correctly captured by the numerical algorithm in order to satisfy the momentum balance at the vicinity of the interface. Readers interested in more details of the PFEM-2 method and the enrichment technique used for the free surface definition may see [11].

The complete analysis requires two steps: during the first one, the two-dimensional Navier-Stokes equations are solved for those Re_D and Fr_D values that finally reach a steady or periodic state $(\overline{\mathbf{v}}, \overline{p}, \overline{\phi})$ known as base flow. For those cases where the Reynolds number is above the critical value and no steady state is obtained (e.g. periodic case), a time averaged solution is analyzed [12] and the result will be confirmed by DMD analysis. During the second step, the base flow (steady or averaged) is perturbed with small wave like ansatz for velocity and pressure such that:

$$\mathbf{v} = \overline{\mathbf{v}} + \varepsilon\widehat{\mathbf{v}}\exp(\omega t) \qquad p = \overline{p} + \varepsilon\widehat{p}\exp(\omega t), \tag{5}$$

where $\varepsilon \ll 1$ and $\omega = \omega_r + i\omega_i$ is a complex number that contains the growth rate (ω_r) and the oscillation frequency (ω_i) of the perturbations. The stability analysis of the equations implies the linearization of

the Navier-Stokes equations around a steady or mean base flow. This process has been done following the same methodology explained in [13] which implies the resolution of a large generalized eigenvalue problem by an iterative Arnoldi method. The baseflow can be considered unstable when any of the ω_r are positive. Note that when the Navier-Stokes equations are solved and perturbed, new terms coming from the α and β gradients may become important and that these have been taken into account on free surface proximities. In addition, two important considerations should be remarked when the analysis is performed:

- For subcritical Reynolds numbers, the steady baseflow implies a final distribution of both fluids determined by the values of the VOF function. The VOF function distribution is not perturbed for the analysis, assuming that the vortex shedding will be the cause of instability. This is later confirmed by DMD analysis.
- For supercritical cases, where the baseflow is unsteady, either a frequency damping algorithm or an averaged process is required to obtain a baseflow suitable for analysis [12, 14]. In our case, the linear global stability analysis is performed on an averaged baseflow. Results are confirmed by an unsteady DMD analysis using no less than 10 snapshots per period.

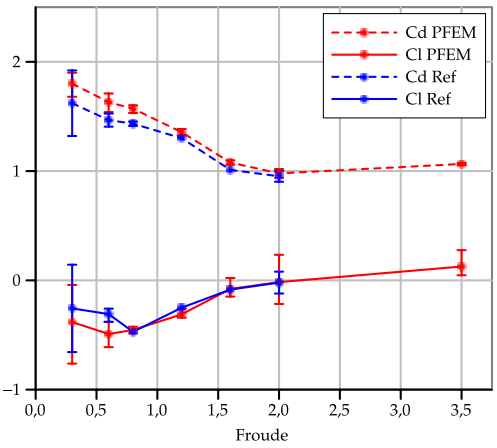

FIG. 2: Drag and lift coefficients calculated with PFEM-2 at $Re_D = 180$ and $h/D = 0.55$ for different Fr_D numbers, comparison with Bouscasse [3].

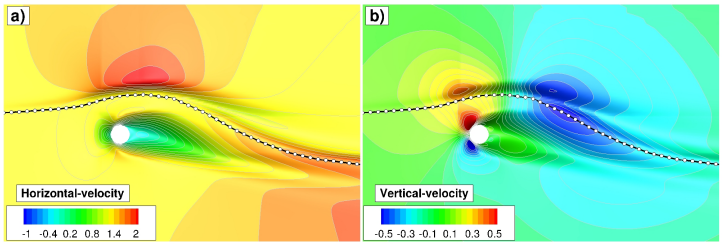

FIG. 3: Steady state solution for $Re_D = 45$, $h/D = 0.55$ and $Fr_D = 3$

RESULTS

For the case where the liquid (bottom fluid) density and fluid viscosity is 100 times their respective top fluid value, we have analyzed a range of Reynolds $Re = (30, 70)$ in the proximities of Re_c. The Froude number has been kept fixed to $Fr_D = 3$ and three different water depth values were studied $h/D = 0.55, 1, 2$. Despite the Reynolds number difference, the free surface elevation at the top of the cylinder is similar to the one presented by Bouscasse [3]. For the sake of validation, the global drag and lift forces have been compared against previous results[3] at the standard $Re_D = 180, h/D = 0.55$ and different Froude numbers being the agreement very satisfactory, see FIG. 2.

For the stability study, a collection of steady baseflows has been obtained varying the Reynolds number and the cylinder depth. An example is provided in FIG. 3, where the horizontal and vertical velocity components of the baseflow (including the free surface location) are shown for $Re_D = 45$, $Fr_D = 3$ and $h/D = 0.55$. For each baseflow, an eigenvalue problem is solved to obtain the most unstable modes. The evolutions of the growth/damping rate and the angular frequencies of the resulting most unstable mode are shown in FIG. 4, where the value without free surface (but with gravity) $h/D = \infty$ is included as a reference (black dot). It can be observed that the most unstable mode moves towards the unstable region $\omega_r < 0$ when the Reynolds number is increased, similarly to what happens in the absence of free surface and gravity (classic result). For Reynolds numbers close to the one found in the absence of free surface and gravity $Re_c \approx 47$, the mode turns to be unstable and vortex shedding process develops. This critical Reynolds value depends on the h/D parameter, increasing when h/D decreases. Note that the $h/D = \infty$ case (black dot in FIG. 4) suggests that gravity is not responsible for the stabilizing effect, which is attributed to the presence of the free surface. This provides a first evidence that the free surface presence increases the stability of the flow. Additionally, an increasing frequency is appreciated by the presence of the gravity field, being the critical frequencies for all cylinder depths noticeably higher that the one associated to the classical case without both free surface and gravity $\omega_c = 0.7414$. We can conclude that the free surface modifies significantly the growth rate but that both gravity and free surface affect the vortex shedding frequency. In addition, let us note that the frequency associated to

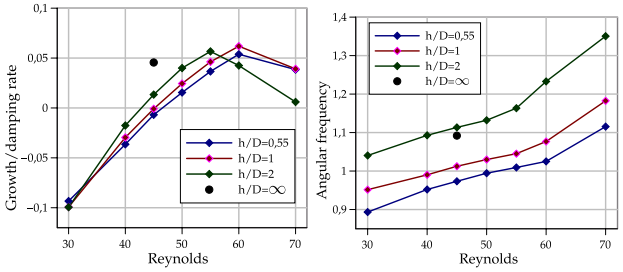

FIG. 4: Growth rate and frequency for varying Re numbers and h/D values. The black dot represents the case with gravity but without free surface ($h/D = \infty$). The classic result in the absence of free surface and gravity has $Re_c = 47$ and $\omega_c = 0.7414$ as critical values.

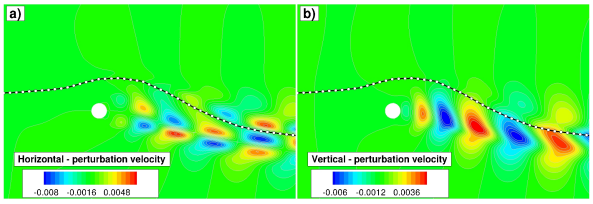

FIG. 5: Unstable mode (real part) for the case $Re = 45$ $Fr_D = 3$ and $h/D = 0.55$

this oscillating unstable mode increases with the cylinder depth. For $h/D = 2$, the frequency is very close to the single phase case with gravity. Therefore, it may be argued that for depths larger than 2 ($h/D > 2$), the free surface presence does not affect significantly the shedding frequency. For these large depths, only the effect of gravity is responsible of variations in frequency.

The mode corresponding to this leading unstable mode for the case $Re_D = 45$ $Fr_D = 3$ and $h/D = 0.55$ is depicted in FIG. 5, where the shape of the mode is visibly influenced by the free surface modulation.

Finally, to confirm the results for the averaged baseflows (supercritical Reynolds), an unsteady DMD analysis has been performed for each cylinder depth. FIG. 6 compares the critical frequencies for the DMD analysis and the averaged baseflow global stability analysis. It can be seen that the values of the frequencies agree well. In all cases the leading frequency is attributed to the vortex shedding phenomena aft the cylinder.

This work has presented for the first time global stability analysis results for a submerged cylinder. These results have shows that the presence of the free surface has a stabilising effect on the onset of vortex shedding and associated von Kármán vortex street. In addition, the free surface and the the gravity field have shown to modify the frequency of shedding. Using the presented methodology, future work will examine growing instabilities caused by the free surface oscillations, as found responsible for Rayleigh-

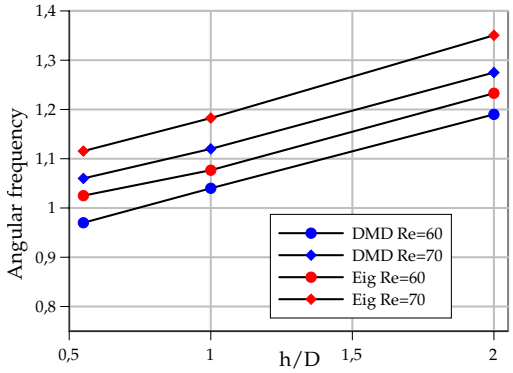

FIG. 6: Critical frequencies for varying cylinder depths and two Reynolds numbers: global analysis of averaged baseflow and DMD.

Taylor type instabilities. This work was supported by the Technical University of Madrid by the project (PID) "Combination of Eulerian and Lagrangian methodologies for the solution of free surface flows."

[1] G. S. Triantafyllou and A. A. Dimas, Physics of Fluids A **1** (1989).
[2] P. Reichl, K. Hourigan, and M. Thompson, Journal of Fluid Mechanics **533**, 269 (2005).
[3] B. Bouscasse, A. Colagrossi, A. Souto-Iglesias, and S. Marrone, in *33rd International Conference on Ocean, Offshore and Arctic Engineering* (2014).
[4] C. P. Jackson, Journal of Fluid Mechanics **182**, 23 (1987).
[5] M. Provansal, C. Mathis, and L. Boyer, Journal of Fluid Mechanics **182**, 1 (1987).
[6] C. H. K. Williamson, Physics of Fluids **31** (1988).
[7] G. Miller and C. Williamson, Experiments in Fluids **18**, 26 (1994).
[8] S. Ohring and H. J. Lugt, Journal of Fluid Mechanics **227**, 47 (1991).
[9] J. Fontane and L. Joly, Journal of Fluid Mechanics **612**, 237 (2008).
[10] C. W. Hirt and B. D. Nichols, Journal of computational physics **39**, 201 (1981).
[11] J. Gimenez and L. González, Journal of Computational Physics **284**, 186 (2015).
[12] D. Sipp and A. Lebedev, Journal of Fluid Mechanics **593**, 333 (2007).
[13] L. González and V. Theofilis and R. Gómez-Blanco, AIAA Journal **45**, 840 (2007).
[14] B. E. Jordi, C. J. Cotter, and S. J. Sherwin, Physics of Fluids (1994-present) **27**, 094104 (2015).
[15] P. Schmid, Journal of Fluid Mechanics **656**, 5 (2010).